Laboratory Measurements of Axial Pressures in Two-Celled Tornado-like Vortices

RANDAL L. PAULEY

Department of Earth and Atmospheric Sciences, Purdue University, West Lafayette, Indiana

(Manuscript received 27 February 1989, in final form 27 June 1989)

ABSTRACT

An experimental study of two-celled vortex flows was conducted in a Ward-type tornado vortex chamber (TVC). Time-averaged, stream-static pressure measurements on the vortex axis and observations of the visualized flow in two-celled vortices are reported. The static pressure measured on the vortex axis increases with height downstream of the vortex breakdown, with the axial pressure gradient tending to zero only well aloft. Visualization indicates that the flow downstream of the breakdown in the TVC is everywhere two-celled, with the strongest axial downflow occurring at middle levels. Analysis of the vertical momentum equation strengthens the argument that the turbulent stresses can play an important role in the axial momentum balance of two-celled vortices by opposing the "filling" of the vortex core with higher stagnation pressure fluid from aloft, therefore helping to maintain low pressure and high velocities near the surface.

1. Introduction

Circumstantial and observational evidence suggests that many columnar atmospheric vortices may have two-celled meridional circulations; a two-celled vortex being defined as one with a stream surface dividing an outer cell of swirling inflow and upflow from an inner cell which may have downflow near the axis. Such circulations have been reported in dust devils (Sinclair 1973) and waterspouts (Golden 1974) and appear prominently in many laboratory and numerical simulations of atmospheric vortices (e.g., Ward 1972; Rotunno 1984; Walko and Gall 1986). Indirect evidence of two-celled flow in tornadoes is cited in Walko (1988), Davies-Jones (1986), and Pauley and Snow (1988). Of particular interest in the case of tornadoes, the nature of the flow on the axis of a vortex has important consequences for the energetics of the flow and maintenance of a large pressure drop (Walko 1988 and references therein), and for the development of a zone of large shear and high vorticity conducive to the formation of subsidiary vortices (Rotunno 1984).

This paper presents results of a laboratory investigation of two-celled columnar vortex flows in a Ward-type tornado vortex chamber [for background on laboratory vortex modeling in a Ward-type TVC the reader is referred to Church et al. (1979)]. These results include time-averaged, stream-static pressure measurements on the vortex axis and observations of the visualized flow in the vortex core. The axial pressures and velocities are then discussed in terms of the axial momentum equation. The principal goal of this work is to better define the vertical momentum balance in the cores of two-celled laboratory vortices. This in turn may help improve our insight into the relation between laboratory vortices and their atmospheric counterparts, and perhaps provide guidance for the development of improved numerical models.

Church and Snow (1985) have previously reported measurements of axial pressures in the lower portions of TVC vortices. Their experiments focused on single-celled flows and employed a technique to compensate for vortex wander by measuring temporal extrema in the pressure deficits. It should be emphasized that the time-*averaged* pressure measurements reported here differ from the time-*dependent* pressure deficits described in the study of Church and Snow (1985). The time-dependent measurements are a good way to account for vortex wander in single-celled flows, but for the two-celled vortices under investigation here, vortex wander is not a significant problem. Neither the time-averaged nor the time-dependent method will give a faultless representation of the pressure distribution if there is significant unsteadiness in the flow; in the absence of vortex wander, however, a time-averaged measurement may yield more representative overall spatial gradients than would the technique based on the time-dependent extrema. For the purposes of this investigation then, a time-averaged measurement was preferred. A more detailed description of the pressure measurement technique is included in section 2.

2. Experimental techniques

The experiments were conducted in the Purdue University TVC I; this apparatus and its operation are

Corresponding author address: Dr. Randal L. Pauley, Laboratory for Computational Physics and Fluid Dynamics, Naval Research Laboratory, Code 4410, Washington, DC 20375.

described in detail in Church et al. (1977) and Church et al. (1979). The only substantial alteration of the TVC for this work was the addition of a cylindrical wall at the radius of the updraft hole surrounding the convection zone (see Fig. 1). This modification facilitated other measurements not reported here and also had the effect of improving the geometric similarity between the laboratory flow and numerical models of the TVC. A single geometry was used, with an inflow depth $h = 0.305$ m, an updraft radius $r_0 = 0.61$ m, and a convection zone depth $l = 0.945$ m. The important similarity parameters characterizing the flow (the swirl ratio S, the radial Reynolds number Re_r, and the aspect ratio a) and other relevant symbols are defined in the Appendix. When not otherwise indicated, methods of measuring flow parameters are similar to those described in earlier papers (e.g., Church and Snow 1985).

a. Axial pressure measurement

The measurement of the static pressure in the interior of turbulent laboratory flows is known to be subject to large uncertainties (Bradshaw 1971), mainly due to the complex interaction of the fluctuating flow with a necessarily intrusive pressure probe. Neglecting viscous effects and assuming the probe is properly aligned with the mean flow, errors arise primarily from cross-flow fluctuations and axial-flow fluctuations (Fuchs 1972). The axial-flow fluctuations are the lesser influence and depend on the placement of the sensing ports on the probe body as well as the level of turbulence. The effect of cross-flow fluctuations is to lower the mean static pressure measured by the probe, and this error depends on both the character of the flow and the turbulence intensity. It is not possible to predict the errors in static pressure measurement for the particular flows in the TVC a priori, so the approach taken was to compare the results of different measurement techniques. Agreement between measurements made by different methods would suggest that the errors, though still unquantified, fall within acceptable limits.

First, axial pressures were measured using a variety of standard pitot-static probes. The static ports of the pitot tubes were connected to a variable-reluctance differential-pressure transducer which had been calibrated against a liquid micromanometer. The reference pressure was taken on the lower wall of the confluence zone at large radius. The output voltage of the pressure transducer was passed through a first-order active filter with a 10-s time constant to obtain time-averaged pressures. Care was taken to ensure that the pressure-measuring system was slightly overdamped (Pauley et al. 1982). As long as the flow is axisymmetric, the mean flow direction on the vortex axis will be vertical, but the sense of the motion is sometimes uncertain in two-celled flows. Consequently, both upward and downward orientations of the pitot probes were checked. Overlapping readings were taken with the various probes. No significant or systematic differences were apparent in the measurements between different-sized tubes, between Prandtl and straight probes, or between opposing orientations of the probes. This suggests that errors due to axial-flow fluctuations and those due to viscous effects—which depend on the size and shape of probe—were not very large.

Another measurement technique made use of a 6-cm diameter cylinder that could be installed on the central axis of the TVC and removed at will. The cylinder was fitted with an array of pressure taps and extended vertically over the entire depth of the chamber and through the baffle. In this instance a scanning-valve assembly was used in conjunction with the same pressure transducer, reference pressure, and signal filtering described above. Flow visualization indicated that the presence of this cylinder had a minimal effect on the morphology of the two-celled vortices. Experimental variation of the azimuthal orientation of the

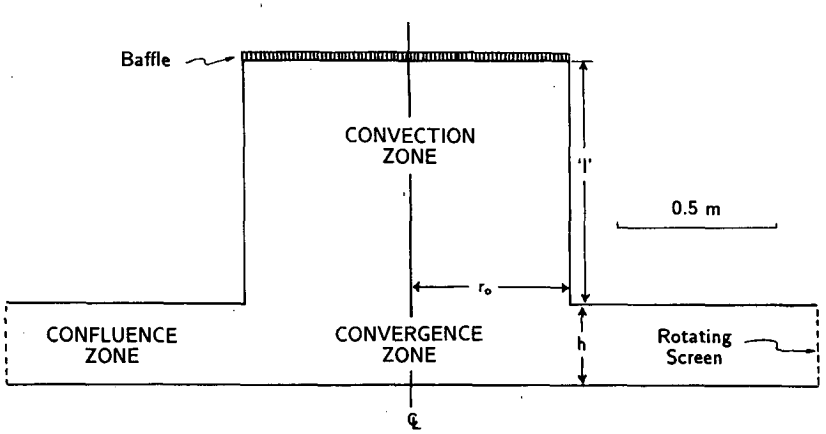

FIG. 1. Modified configuration of the Purdue TVC I with the outer wall of the convection zone at $r = r_0$. Compare with Fig. 2 in Church et al. (1979).

pressure taps revealed little evidence of significant asymmetry in the mean flow near the axis.

It seems reasonable that the fluctuating flow should interact very differently with the central cylinder, which provides a nearly wall-static reading, than it does with the small pitot-static tubes. One would then expect errors of dissimilar magnitudes for the two measurement techniques. However, the pressures measured on the surface of the cylinder and those measured with the pitot-static probes turned out to be in remarkable accord. The only significant differences arose very near the surface where the physical presence of the cylinder most disrupted the flow. Admittedly, both measurement techniques are subject to systematic errors in the same direction, but considering that the character of the flow (and the turbulence) varies with height in the vortex, the close agreement of the two methods over the full depth of the TVC suggests that systematic errors are not too large. The good agreement between measurement techniques may be attributable to low levels of turbulent cross-flow fluctuations on the vortex axis. The *relative* turbulence intensity on the axis is large because the mean flow is weak, but flow visualization and exploratory measurements using hot-film anemometry both suggest that the *absolute* turbulence intensity on the axis is not too great in most cases. Consequently, the errors in the stream-static pressure measurements appear to be relatively small.

b. *Velocity observations*

Quantitative measurements of the flow velocity using conventional hot-film anemometry were rendered inaccurate by the low velocities, high relative turbulence intensities, and concomitant high rates of instantaneous flow reversal encountered in the cores of the two-celled TVC vortices. As an alternative, flow visualization was used to provide a qualitative picture of the flow on and near the vortex axis. The routine flow visualization in the Purdue TVC I entailed the release of kerosene fog into the surface boundary layer feeding the vortex core. The fog was supplied to the flow from beneath the edge of a thin circular disk elevated a few millimeters above the lower surface. Fog was also dumped into the plenum above the baffle and could be drawn downward into the core of a two-celled vortex. However, this visualization proved inadequate to clearly and consistently delineate the flow near the vortex axis.

Two methods were developed to improve the flow visualization in the core. First a 3.3-cm diameter tube was placed on the centerline of the TVC in a similar fashion to the cylinder fitted with pressure taps mentioned above. This tube, however, was drilled with a series of small holes to allow the release of filaments of flow-visualizing fog. The fog was supplied to the tube from beneath the chamber and its volume flow rate could be controlled to assure a gentle entry into the flow. As with the pressure-measuring cylinder, the two-celled vortices were little affected by the presence of the tube except for some slight disruption of the flow near the surface. Then, to obtain a more accurate picture of the flow in the lower part of the vortex, this tube was removed and a single filament of fog was supplied to the axis via a 4-mm diameter tube inserted into the flow from underneath the chamber. This small tube had a 90° elbow so that the fog was released with no vertical momentum. The position of the tube could be adjusted vertically to visualize the flow with minimal disturbance. This flow visualization allowed a determination of the axial flow direction and qualitative estimation of the vertical flow speed and level of turbulent fluctuations.

It is hoped that in the next generation of Ward-type TVC, laser anemometry will facilitate velocity measurements that will more fully and accurately detail the structure of two-celled vortex cores. For example, the present results do not include data on the tangential velocity field, which would be useful in examining the cyclostrophic contribution to the axial pressure and its development with height. Also lacking are the quantitative measurements of the meridional velocities and the turbulent velocity correlations that could better define the core dynamics and provide a benchmark for testing numerical models.

3. Results

The experiments detailed here were conducted at an aspect ratio $a = 0.5$, a radial Reynolds number $\mathrm{Re}_r = 1.65 \times 10^4$, and swirl ratios of $S = 0.6$ and 0.85. Standard flow visualization revealed the following vortex morphologies for these flow conditions.

- At $S = 0.6$ a vortex breakdown was very near the surface but still identifiable. Vortex breakdown is the abrupt transition from a single-celled vortex with a jetlike vertical velocity profile to a two-celled vortex with a wakelike vertical velocity profile (Hall 1972). The vortex morphology with a breakdown at the surface is sometimes termed an endwall breakdown or a "drowned vortex jump." The transition to two orbiting subsidiary vortices was just beginning to take place aloft at this swirl ratio.
- When the swirl ratio was increased to $S = 0.85$, a more or less persistent "eye" developed in the corner region at the surface as the boundary layer erupted before reaching the axis. The two orbiting subsidiary vortices were well established, extending near, and transiently penetrating to, the surface.

The results of the release of flow-visualizing fog on the axis of the vortex are summarized in Table 1. Height is nondimensionalized here by the inflow depth h, with the convection zone terminating at $Z \equiv z/h = 4.1$. In the upper portion of the convection zone the axial flow

TABLE 1. Vertical flow on the vortex axis as a function of nondimensional height.

	$S = 0.6$	$S = 0.85$
I Nearly stagnant or weak downflow	$Z > 3$	$Z > 2.5$
II Accelerating and/or strong downflow	$1.5 < Z < 3$	$0.5 < Z < 2.5$
III Decelerating and/or moderate downflow	$0.1 < Z < 1.5$	$Z < 0.5$
IV Intermittent upflow and downflow	$Z < 0.1$	—

was quite weak in both cases, with gentle subsidence indicated in the mean (regime I). In the middle levels of the TVC this downflow was accelerated into a fairly vigorous downdraft (regime II). In the lower reaches of the vortex the downflow was gradually decelerated to zero at or near the surface (regime III).

In the endwall breakdown flow ($S = 0.6$) the vertical flow direction in the corner region ($Z < 0.1$) was rather unsteady (regime IV). The vortex breakdown was observed to oscillate up and down slightly in this flow regime. The intermittency in the vertical flow direction then arises because the flow upstream of the breakdown is upwards while the flow on the axis downstream of the breakdown is downward. Although there may be complex circulations *within* the breakdown, no return to mean upflow on the axis was observed at any point downstream of the breakdown. This was confirmed not only for the particular cases at hand, but for a wide range of flow conditions.

Figures 2 and 3 show vertical distributions of time-averaged, stream-static pressure deficit on the axis of the TVC for $S = 0.6$ and 0.85, respectively. Following Pauley et al. (1982), pressures are nondimensionalized by ρw_0^2, where w_0 is the mean updraft speed in the convection zone.[1] The data shown are pitot-static measurements made *without* the central cylinder in place. The solid circle indicates the centerline surface pressure deficit while the open circle gives the axial pressure deficit at the top side of the flow-straightening baffle. The Roman numerals designate the axial velocity regimes as defined in Table 1.

In the upper reaches of the $S = 0.6$ vortex (Fig. 2) the axial pressure is approximately constant with height. This constant pressure region corresponds well with the nearly stagnant or weakly subsiding axial velocity regime (I). Below about $Z = 2.5$ the axial pressure

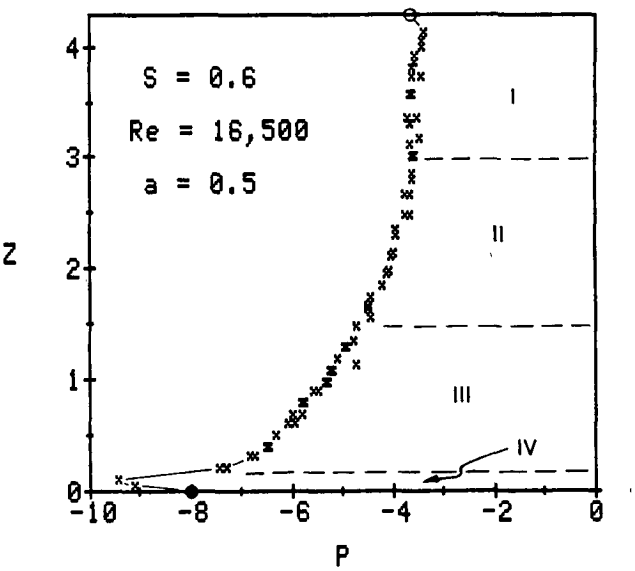

FIG. 2. Nondimensional stream-static pressure deficit versus nondimensional height on the central axis of the TVC for $S = 0.6$. The solid circle indicates the centerline surface pressure while the open circle gives the axial pressure at the top side of the flow-straightening baffle. Roman numerals designate the axial velocity regimes described in Table 1.

gradient becomes increasingly adverse.[2] Axial velocity regimes II and III, both with identifiable downdrafts, are fairly well encompassed by the region of adverse axial pressure gradient. There is a pronounced pressure minimum near the surface in the vicinity of the vortex breakdown. Upstream of the breakdown just above the surface there is a favorable axial pressure gradient; this gives way to an adverse gradient downstream of the breakdown. The flow is unsteady here with the vortex breakdown oscillating up and down, so the time averaging tends to lessen the actual pressure gradients. The intermittent axial velocity regime (IV) with fluctuating upflow and downflow accompanies this region in which the pressure gradient changes sign. The large instantaneous pressure deficits in the single-celled flow just upstream of the breakdown were a focal point in the work of Church and Snow (1985). These large time-dependent deficits, however, tended to obscure the character of the axial pressure in the two-celled portion of the flow downstream of the breakdown, which appeared in comparison to be nearly uniform with height

[1] It was discovered during this investigation that an inaccurate calibration of the TVC flow rate had been used for some previous work. Consequently, the results published in Pauley et al. (1982) have systematic errors of about +15% in the Reynolds number and −24% in nondimensional pressures. These errors, however, do not affect the conclusions drawn in that paper.

[2] Under the convention adopted here an "adverse" axial pressure gradient is one in which the pressure increases with height, while a "favorable" axial pressure gradient is one in which pressure decreases with height. "Adverse" and "favorable" then denote the relation of the pressure gradient to the overall throughflow—which is always upward. These terms as used here do not refer to the relation between the pressure gradient and the *local* flow direction on the axis—which might be downward.

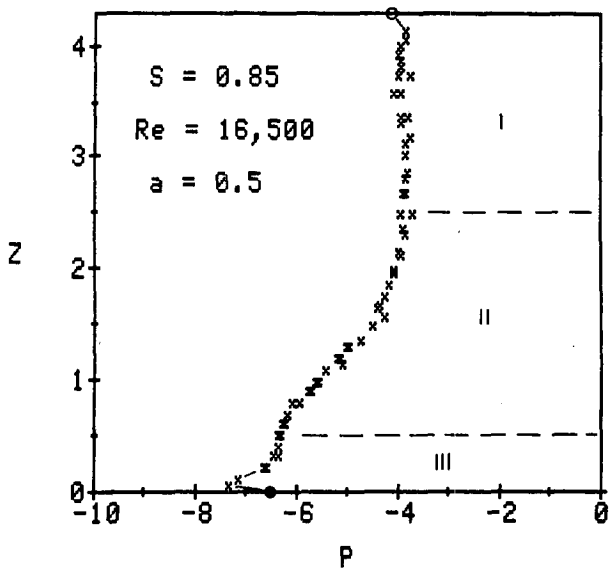

FIG. 3. Same as Fig. 2 except $S = 0.85$.

(see Fig. 3 of Church and Snow 1985). The time-averaged measurements shown in Fig. 2 indicate a very abrupt change in pressure at the breakdown, but also reveal a significant region aloft with a very definite adverse pressure gradient.

The axial pressure distribution for the multiple vortex flow ($S = 0.85$) shown in Fig. 3 shares some common features with the endwall vortex breakdown flow. The region of nearly zero pressure gradient is again apparent in the upper portion of Fig. 3, but here extends to somewhat lower levels in the vortex. We also see a similar correlation between this region of constant pressure and the nearly stagnant axial flow regime (I). An adverse axial pressure gradient is again present in the middle levels of the TVC corresponding roughly to the region of accelerating downdraft (II).

Setting aside for a moment the pressure minimum just above the surface, there seems to be a tendency to a less adverse pressure gradient below about $Z = 0.7$ in this multiple vortex flow. This is approximately coincident with the decelerating axial velocity regime (III). Indeed, except for the two lowest stream-static measurements, the axial pressure profile appears to asymptotically approach the surface value of $P = -6.5$. This reduction in the axial pressure gradient in the convergence zone is also observed in measurements made for $S = 0.95$ (not shown).

The pressure minimum just above the surface for $S = 0.85$ might be associated with unsteady features in the near-surface flow. For example, unsteadiness in the surface "eye" structure may have included transient return to endwall vortex breakdown conditions—a circumstance that can be difficult to judge visually. Flow visualization also indicated some unsteadiness in the orbiting subsidiary vortices, although it was not clear if they approached near enough the axis at this level to influence the measurement. However, it is also possible that this pressure minimum may be an artifact of the measurement technique, which is more prone to error when the flow fluctuations are large—due to either turbulence or unsteadiness in the flow.

4. Discussion

Consider the dimensional form of the Reynolds-averaged vertical momentum equation near the axis of a steady, axisymmetric, incompressible, quasi-cylindrical vortex:

$$\underset{\text{(A)}}{\frac{\partial}{\partial z}\frac{\bar{w}^2}{2}} = \underset{\text{(B)}}{-\frac{1}{\rho}\frac{\partial \bar{p}}{\partial z}} + \underset{\text{(C)}}{\frac{\nu}{r}\frac{\partial}{\partial r}\left(r\frac{\partial \bar{w}}{\partial r}\right)} - \underset{\text{(D)}}{\frac{1}{r}\frac{\partial}{\partial r}(r\overline{u'w'})}, \quad (1)$$

where the overbars and primes denote time averaged and fluctuating components, respectively. This equation follows simply from the derivations for a quasi-cylindrical vortex core in Hall (1966) when it is recognized that $\bar{u} \to 0$ near the axis and when the additional assumptions of steady flow and incompressibility are invoked. In a flow with subsidiary vortices, the axisymmetric assumption is only valid over relatively long time scales; close to the axis, however, the flow appears to remain essentially axisymmetric over much shorter time scales. In addition to axisymmetry, the quasi-cylindrical approximation assumes that radial gradients are much larger than vertical gradients and that fluctuating velocities are generally small compared to mean velocities. This approximation is not completely valid for the two-celled vortices in the TVC, but the terms eliminated by invoking it should not greatly alter the simple physical arguments to be presented here.

Term A in (1) can be interpreted either as a vertical acceleration or a vertical momentum flux term. The axial pressure gradient force is given by term B. Terms C and D are viscous and turbulent shear stress divergences, respectively. In turbulent flow the viscous stresses are negligible compared with the eddy stresses, so term C can be dropped.

Term A is negative when the downdraft is accelerating, positive when it is decelerating. An adverse pressure gradient corresponds to term B negative, a favorable pressure gradient to term B positive. So long as the strongest downflow is on the axis (i.e., the vertical velocity profile is wakelike), term D should be positive.

The sign of the axial pressure gradient (term B) as a function of height is known from measurement; from flow visualization we can infer the sign of the vertical momentum flux or acceleration (term A) as a function of height; and for a two-celled flow with a simple, wakelike, mean vertical velocity profile, we can deduce that the sign of the turbulent shear stress divergence

term near the axis is positive. Knowing the signs of the various terms over different levels in the vortex, it is then possible to draw some inferences about the vertical momentum balance in the vortex core.

Consider the axial momentum balance in the four flow regimes or regions delineated in Fig. 2 for the endwall vortex breakdown ($S = 0.6$). In region I none of the terms in the axial momentum equation is significantly nonzero. The vertical flow is almost stagnant, the pressure is nearly constant with height, and the eddy stress term likewise must be small for the equation to balance. The latter is consistent with a broad core flow in which the radial gradients near the axis are weak.

In region II terms A and B are both negative as the downflow accelerates and the pressure gradient is adverse. The eddy stress term is nonzero and positive since the radial gradient of vertical velocity becomes stronger as the axial downflow accelerates. The primary balance in the axial momentum equation would appear to be between the adverse pressure gradient and the accelerating downflow. Insufficient quantitative information is available to evaluate the relative magnitude of the eddy stress term, though it may contribute toward a weakening of the downward acceleration and/or a strengthening of the adverse pressure gradient.

The axial momentum balance in region III is quite different. Here the downflow is decelerating so term A is positive, but the pressure gradient is even more adverse than in region II so term B is strongly negative. For the momentum equation to balance then, the eddy stress term must be strongly positive. So the primary balance in region III appears to be between the pressure gradient force and the turbulent shear stress divergence. This is analogous to the axial momentum balance in turbulent pipe flow, as described by Ward (1972) and Baker and Church (1979). The relative motion between the descending axial flow and the rapidly ascending flow in the outer cell of the vortex is similar to that between the fluid flowing in a pipe and the stationary pipe wall. The transport of vertical momentum from the outer cell toward the axis of the vortex represented by term D in (1) is then analogous to the radial transport of axial momentum defect from the wall toward the centerline in turbulent pipe flow. The effect of this frictional term is to resist the "filling" of the vortex core with higher stagnation pressure fluid from aloft, and so help to maintain a low pressure near the surface. This is a nonhydrostatic effect (so the term "filling" is used advisedly) and is analogous to the head loss that occurs in turbulent pipe flow.

The flow in region III might also be influenced by the normal component of the turbulent stress divergence, a term that is eliminated from the momentum equation by invoking the quasi-cylindrical approximation. This term, would otherwise appear alongside the turbulent shear stress divergence in (1). Based on the flow visualization, the normal turbulent stress is most likely to be nonnegligible here in region III, where the turbulence intensities are large. Qualitatively, the flow visualization suggests that the normal turbulent stress term in this region probably has the same sign as the turbulent shear stress term, so that both would oppose "filling" of the vortex core. A more definitive analysis of the relative strength of these terms will require quantitative measurements of the turbulent velocity correlations.

Considering region IV, Wilson and Rotunno (1986) have shown that near the surface in a single-celled vortex the upward acceleration of the axial flow almost precisely balances the favorable axial pressure gradient. This may be a fair approximation of the flow field upstream of the breakdown in the endwall vortex breakdown configuration, though no conclusions can be drawn from the data available here.

In the multiple vortex flow ($S = 0.85$) the balances of axial momentum in the three regions delineated in Fig. 3 do not appear to differ much from the corresponding regions in the case of the endwall vortex breakdown discussed above. However, the extent of the "turbulent pipe flow" region (III) is reduced and the accompanying axial pressure gradient is less adverse in the higher-swirl flow. This is probably related to the expansion of the vortex core with increasing swirl. Radial gradients of vertical velocity decrease as the core expands and so too does the turbulent shear stress divergence, inhibiting the establishment of a strong adverse pressure gradient on the axis.

The flow in tornadoes and other geophysical columnar vortices is obviously much more complex than that in the TVC. One of the important physical effects relevant to the axial momentum balance in geophysical vortices is the buoyancy that can arise due to vertical motions in a compressible atmosphere where the potential temperature is a function of height, an effect that is absent in the isothermal laboratory flow. Compressional heating in the axial downdraft of a two-celled tornado, for example, might result in significant hydrostatic unweighting of the vortex core, an effect discussed and investigated at length in Walko (1988). Whether substantial hydrostatic unweighting of the vortex core is required to explain observed maximum tornado windspeeds remains an open question.

The present laboratory results are relevant to the atmospheric problem since they accentuate an important nonhydrostatic mechanism for sustaining low surface pressures and concomitant high windspeeds in a vortex—the turbulent stresses. The presence of a "turbulent pipe flow" regime in a tornado would mitigate, although it would not necessarily obviate, the need for very warm downdrafts to account for observed windspeeds. The somewhat paradoxical role that the eddy stresses may play in tornado dynamics has been recognized by several investigators (Ward 1972; Lew-

ellen 1976; Baker and Church 1979; Walko and Gall 1986; Walko 1988), but its potential significance has sometimes been neglected in previous analyses (e.g., Snow and Pauley 1984).

The character of the turbulence in the vortex core plays a multifaceted role in the present context. Eddy momentum diffusion may be a primary mechanism for driving the axial downdraft in a two-celled vortex (Walko 1988), and the nature of the turbulence will also affect the rate of entrainment into the core and thereby the amount of dilution of any compressionally heated downdraft. Moreover, the presence of large-scale subsidiary vortices may have an important influence on the axial momentum balance by increasing the eddy momentum transport. There is some evidence of this influence in three-dimensional numerical vortex modeling results (cf. Figs. 6 and 10 in Rotunno 1984). Axisymmetric tornado models then may be inadequate to fully address the problem, or at least may require some advanced turbulence parameterization.

Another issue raised in this investigation concerns the vertical extent of the two-celled circulation in the vortex core. While no return to single-celled flow downstream of the vortex breakdown was observed in the TVC vortices, observational evidence suggests that there may indeed be a return to upflow on the axis downstream of vortex breakdown in some tornadoes (Pauley and Snow 1988). At least three factors could contribute to positive vertical forcing on the axis of a two-celled tornado: buoyancy, a favorable pressure gradient associated with either an increase in the ambient circulation with height or stretching of the core vorticity aloft, and the action of turbulent stresses. Of these, only the turbulent stresses are present in the TVC flow. Perhaps in a much taller chamber, the turbulent stresses alone might be sufficient to effect a return to single-celled flow farther aloft. In this connection, the presence of the flow-straightening baffle in the TVC should not preclude such a return to axial upflow downstream of the breakdown.

5. Summary

Time-averaged, stream-static pressure measurements on the vortex axis and observations of the visualized flow in the vortex core have been reported for two-celled vortices in a Ward-type TVC. The axial pressure increased with height downstream of the vortex breakdown, with the pressure gradient tending to zero only well aloft in the convection zone. It is argued that these time-averaged measurements better capture the character of the axial pressure gradients in two-celled vortices, which was somewhat obscure in previous time-dependent data. Visualization indicated that the flow downstream of the breakdown in the TVC is everywhere two-celled, with the strongest axial downflow occurring at middle levels. No evidence was found of a return to single-celled flow downstream of the breakdown.

Analysis of the vertical momentum equation strengthens the argument that the turbulent stresses can play an important role in the axial momentum balance of two-celled vortices by opposing the "filling" of the vortex core with higher stagnation pressure fluid from aloft, and so helping to maintain low pressure and high velocities near the surface. Modeling of the turbulence, probably including the effects of large coherent subsidiary vortex structures, then appears to be an essential element in improved numerical tornado simulation.

Acknowledgments. I would like to thank Drs. J. T. Snow, C. R. Church, D. R. Smith, and W. G. Tiedeman for their counsel on various aspects of this investigation. This material is based upon work supported by the National Science Foundation under Grants ATM 82-03403 and ATM 84-03757.

APPENDIX

Symbols

a	aspect ratio ($\equiv h/r_0$)
h	depth of the confluence zone
l	depth of the convection zone
p	pressure
$\bar{p}$	time-averaged component of pressure
$\bar{p}_{\text{ref}}$	reference pressure ($\bar{p}$ at $r = 1.2$ m, $z = 0$)
$\Delta\bar{p}$	deficit pressure ($\equiv \bar{p} - \bar{p}_{\text{ref}}$)
P	nondimensional deficit pressure ($\equiv \Delta\bar{p}/\rho w_0^2$)
Re_r	radial Reynolds number ($\equiv u_0 r_0/\nu$)
r	radial coordinate
r_0	radius of the updraft hole
S	swirl ratio ($\equiv \Gamma_0/4\pi u_0 h$)
u	radial velocity
$\bar{u}$	time-averaged component of the radial velocity
u'	fluctuating component of the radial velocity
u_0	mean radial velocity at $r = r_0$
v	tangential velocity
w	vertical velocity
$\bar{w}$	time-averaged component of the vertical velocity
w'	fluctuating component of the vertical velocity
w_0	mean vertical velocity in the convection zone ($z \geq h$)
z	vertical coordinate
Z	nondimensional vertical coordinate ($\equiv z/h$)
Γ	circulation ($\equiv 2\pi r v$)
Γ_0	circulation at $r = r_0$
ν	kinematic viscosity
ρ	density

REFERENCES

Baker, G. L., and C. R. Church, 1979: Measurements of core radii and peak velocities in modeled atmospheric vortices. *J. Atmos. Sci.*, **36**, 2413–2424.

Bradshaw, P., 1971: *An Introduction to Turbulence and its Measurement.* Pergamon Press, 218 pp.

Church, C. R., and J. T. Snow, 1985: Measurements of axial pressures in tornado-like vortices. *J. Atmos. Sci.*, **42**, 576–582.

——, J. T. Snow and E. M. Agee, 1977: Tornado vortex simulation at Purdue University. *Bull. Amer. Meteor. Soc.*, **58**, 900–908.

——, ——, G. L. Baker and E. M. Agee, 1979: Characteristics of tornado-like vortices as a function of swirl ratio. *J. Atmos. Sci.*, **36**, 1755–1776.

Davies-Jones, R. P., 1986: Tornado dynamics. *Thunderstorms: A Social, Scientific and Technological Documentary, Volume 2: Thunderstorm Morphology and Dynamics.* E. Kessler, Ed., University of Oklahoma Press, 197–236.

Fuchs, H. V., 1972: Measurements of pressure fluctuations within subsonic turbulent jets. *J. Sound Vib.*, **22**, 361–378.

Golden, J. H., 1974: The life-cycle of Florida Keys' waterspouts. I. *J. Appl. Meteor.*, **13**, 676–692.

Hall, M. G., 1966: The structure of concentrated vortex cores. *Prog. Aeronaut. Sci.*, **7**, 53–110.

——, 1972: Vortex breakdown. *Ann. Rev. Fluid Mech.*, **4**, 195–218.

Lewellen, W. S., 1976: Theoretical models of the tornado vortex. *Proceedings Symposium on Tornadoes,* R. E. Peterson, Ed., Institute for Disaster Research, Texas Tech University, 151–174.

Pauley, R. L., and J. T. Snow, 1988: On the kinematics and dynamics of the 18 July 1986 Minneapolis tornado. *Mon. Wea. Rev.*, **116**, 2731–2736.

——, C. R. Church and J. T. Snow, 1982: Measurements of maximum pressure deficits in modeled atmospheric vortices. *J. Atmos. Sci.*, **39**, 369–377.

Rotunno, R., 1984: An investigation of a three-dimensional asymmetric vortex. *J. Atmos. Sci.*, **41**, 283–298.

Sinclair, P. C., 1973: The lower structure of dust devils. *J. Atmos. Sci.*, **30**, 1599–1619.

Snow, J. T., and R. L. Pauley, 1984: On the thermodynamic method for estimating maximum tornado windspeeds. *J. Climate Appl. Meteor.*, **23**, 1465–1468.

Walko, R. L., 1988: Plausibility of substantial dry adiabatic subsidence in a tornado core. *J. Atmos. Sci.*, **45**, 2251–2267.

——, and R. L. Gall, 1986: Some effects of momentum diffusion on axisymmetric vortices. *J. Atmos. Sci.*, **43**, 2137–2148.

Ward, N. B., 1972: Exploration of certain features of tornado dynamics using a laboratory model. *J. Atmos. Sci.*, **29**, 1194–1204.

Wilson, T., and R. Rotunno, 1986: A numerical simulation of a laminar end-wall vortex and boundary layer. *Phys. Fluids*, **29**, 3993–4005.